

## CARBON DIOXIDE AND METHANE FLUXES IN THE LITTORAL ZONE OF A TROPICAL SAVANNA RESERVOIR (CORUMBÁ, BRAZIL)

Ivan Bergier<sup>1\*</sup>, Evelyn M. L. M. Novo<sup>2</sup>, Fernando M. Ramos<sup>2</sup>, Edmar A. Mazzi<sup>3</sup> & Maria F.F.L. Raseira<sup>3</sup>

<sup>1</sup> Embrapa Pantanal, Rua 21 de Setembro, 1880, Corumbá, MS, Brasil. CEP: 79320-900.

<sup>2</sup> Instituto Nacional de Pesquisas Espaciais, Avenida dos Astronautas, 1758, São José dos Campos, SP, Brasil. CEP: 12227-010.

<sup>3</sup> Centro de Energia Nuclear na Agricultura, Avenida Centenário, 303, Piracicaba, SP, Brasil. CEP: 13400-970.

E-mails: ivan@cpap.embrapa.br, evlyn@dsr.inpe.br, fernando.ramos@inpe.br, eamazzi@cena.usp.br, mraser@cen.usp.br

### ABSTRACT

A series of dynamic chambers, an infrared photoacoustic gas analyzer and atmospheric and water quality sensors were deployed to determine CH<sub>4</sub> and CO<sub>2</sub> emissions and related environmental conditions in Corumbá Reservoir, Goiás, Brazil. Mean CH<sub>4</sub> bubble fluxes in November 2004, and March and August 2005 were 0.05 ± 2.19, 4 ± 45 and 505 ± 1192 mgCH<sub>4</sub>.m<sup>-2</sup>.d<sup>-1</sup>, respectively. Mean CH<sub>4</sub> diffusive fluxes were 17 ± 6, 37 ± 9 and 69 ± 28 mgCH<sub>4</sub>.m<sup>-2</sup>.d<sup>-1</sup>, and CO<sub>2</sub> diffusive fluxes were respectively 59 ± 398, 385 ± 629 and 1466 ± 1223 mgCO<sub>2</sub>.m<sup>-2</sup>.d<sup>-1</sup>. Gas fluxes varied according to the depth of the sampling sites in the littoral zone, though spatial or temporal patterns were not seasonally consistent. Changes in CH<sub>4</sub> and CO<sub>2</sub> emissions were likely associated with changes in sediment pressure, methanogenesis and methanotrophy induced by atmospheric and climate variations, such as cold fronts and hydrologic variations.

**Keywords:** Tropical dams; methane; carbon dioxide; photoacoustic-dynamic chambers.

### RESUMO

**FLUXOS DE METANO E DO DIÓXIDO DE CARBONO EM UM RESERVATÓRIO HIDRELÉTRICO DO CERRADO (CORUMBÁ, BRAZIL).** Uma série de câmaras dinâmicas, um analisador photo acústico infravermelho de gás e sensores atmosféricos de qualidade do ar e água foram utilizados para determinar as emissões de CH<sub>4</sub> e CO<sub>2</sub> e assim relacioná-las às condições ambientais no reservatório de Corumbá, Goiás, Brasil. Os fluxos médios de CH<sub>4</sub> por bolhas em novembro de 2004, em março e em agosto de 2005 foram 0.05 ± 2.19, 4 ± 45 e 505 ± 1192 mgCH<sub>4</sub>.m<sup>-2</sup>.d<sup>-1</sup>, respectivamente. Para os mesmos meses, as emissões médias de CH<sub>4</sub> por difusão foram 17 ± 6, 37 ± 9 e 69 ± 28 mgCH<sub>4</sub>.m<sup>-2</sup>.d<sup>-1</sup>, enquanto que os fluxos difusivos de CO<sub>2</sub> foram respectivamente 59 ± 398, 385 ± 629 and 1466 ± 1223 mgCO<sub>2</sub>.m<sup>-2</sup>.d<sup>-1</sup>. Os fluxos de gases variaram de acordo com a profundidade dos pontos de amostragem na zona litorânea, embora os padrões espaciais e temporais não foram sazonalmente consistentes. Mudanças nas emissões de CH<sub>4</sub> e CO<sub>2</sub> estão provavelmente condicionadas por variações na pressão exercida no sedimento, pela metanogênese e pela metanotrofia, as quais são induzidas por variações climáticas e atmosféricas, tais como frentes frias e variações hidrológicas.

**Palavras-chave:** Reservatórios tropicais; dióxido de carbono; metano; câmaras dinâmicas.

### INTRODUCTION

Recent investigations indicate that reservoirs are responsible for net emissions of methane (CH<sub>4</sub>), and are contributing to anthropogenic global warming (St. Louis *et al.* 2000, Duchemin *et al.* 2002, Abril *et al.* 2005). Tropical reservoirs are especially significant

sources of methane, and their importance is likely to increase as more are planned to be constructed. The sediments of tropical reservoirs are usually anoxic providing suitable conditions for methanogenesis during decay of organic matter. The fate of the sediment-derived CH<sub>4</sub> can be the sudden release of methane bubbles or mixing through the water column

to the atmosphere, or bacterial oxidation in the upper oxic layers. Although still uncertain,  $\text{CH}_4$  releases can also occur through spillways and turbines and in downstream rivers (Abril *et al.* 2005, Guérin *et al.* 2006, Lima *et al.* 2008).

Diffusive gas exchange is usually calculated based on thin boundary layer models or measured by closed static chambers (Liss & Slater 1974). Duchemin *et al.* (1999) and Matthews *et al.* (2003) provide a review of these approaches.  $\text{CH}_4$  bubble fluxes are often measured by deployments of inverted funnels (Keller & Stallard 1994, Joyce & Jewell 2003). Chambers with continuous airflow, called dynamic chambers, have been used in soil/air gas efflux measurements (Nay *et al.* 1994, Fang & Moncrieff 1998), but rarely for air/water exchanges (Crill *et al.* 1988, Ramos *et al.* 2006). The basic concept is that the continuous airflow through the chamber allows quasi-instantaneous flux measurement. Care must be taken since improper dynamic chamber designs might result in negative inner pressure and gas efflux overestimation (Fang & Moncrieff 1998). As for static chambers, walls somehow minimize direct influences of the wind. The main advantages are the quasi-continuous monitoring during day and night and the ability to capture episodic bubbling events. Dynamic chambers and infrared photoacoustic detection at water/air interfaces were proposed in Lima *et al.* (2005a) based on the chamber design of Fang & Moncrieff (1998). Analogous approaches using photoacoustic detection were used by Yamulki & Jarvis (1999) and Christensen *et al.* (2003a).

The objectives of this paper are to present quasi-continuous measurements of  $\text{CH}_4$  bubbling and  $\text{CH}_4$  and  $\text{CO}_2$  diffusive fluxes from a tropical reservoir in different seasons and at multiple sites in the littoral zone, and to examine how environmental conditions are related to these fluxes.

## DESCRIPTIONS OF THE STUDY AREA

Corumbá reservoir is located in Goiás, Brazil, on the Corumbá River, an important branch of the Parnaíba River in the Paraná River basin. The reservoir provides hydroelectric power and tourism to the city of Caldas Novas (Figure 1). The Corumbá River drains 27,800km<sup>2</sup> of a warm and humid savanna with

annual mean temperature of about 23°C and extremes between 15 and 35°C. Annual precipitation averages 1500mm, concentrated during the austral summer.

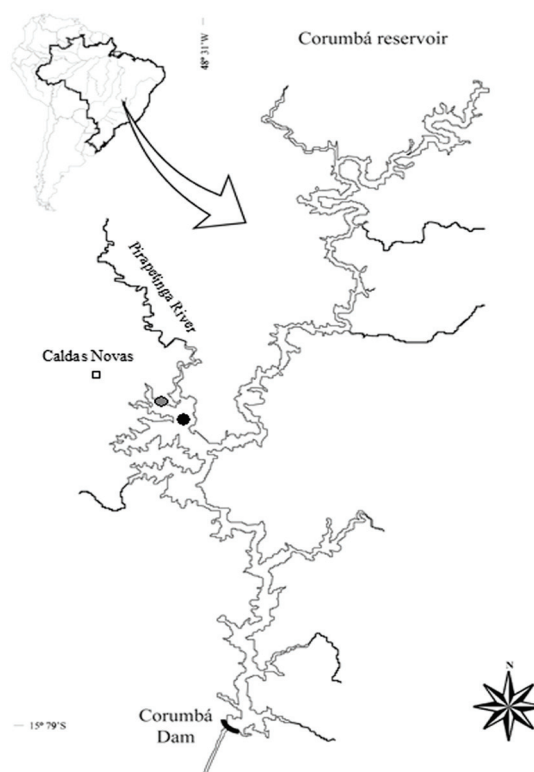


**Figure 1.** Corumbá Reservoir in Goiás, Brazil. The gray circle indicates the site of gas flux measurements in the littoral zone (17°45'56'' S, 48°34'06'' W), and the black circle points to the site of atmospheric and limnologic measurements in the pelagic zone (17°46'40'' S, 48°33'39'' W). Adapted from Felisberto & Rodrigues (2004).

Furnas Centrais Elétricas completed filling the reservoir in 1997, and it normally reaches about 65km<sup>2</sup> in surface area (Figure 1). Three turbines generate 375MW. Maximum water depth varies from 35 to 45m.

## METHODS

### GAS FLUX MEASUREMENTS

During the periods from 21-24 November 2004 and 12-19 March 2005, four floating dynamic chambers were placed at four sampling sites in the littoral zone of Corumbá Reservoir (Figure 1). Depths of the sampling sites were 1.5, 3.0, 3.5 and 6.0m in November 2004 and 0.4, 2.0, 4.0 and 6.0m in March 2005. The chambers were cylindrical, 30cm diameter,

30cm height, and about 10cm below the water surface as a skirt. The top plate was covered with a reflective film to minimize solar heating. A quick-release connector was fitted to the top plate to pump atmospheric air into the chambers. A pipe 25cm in height and 5cm in diameter provided an outlet vent (Figure 2). This design allowed continuous airflow inside the chamber, minimizing temperature increase and pressure decrease. A Charles Austen

Capex-V2<sup>®</sup> pump was connected to a dead volume to drive atmospheric air at a constant airflow rate of ca. 300ml.min<sup>-1</sup> through 90m, 2mm inner diameter nylon tubes connected to each chamber. Similar tubing was used to measure gas exiting chamber outlets. Outlet gas sampling was done via the built-in pump of the gas analyzer, aided by another Charles Austen Capex-V2<sup>®</sup> pump (Figure 2).

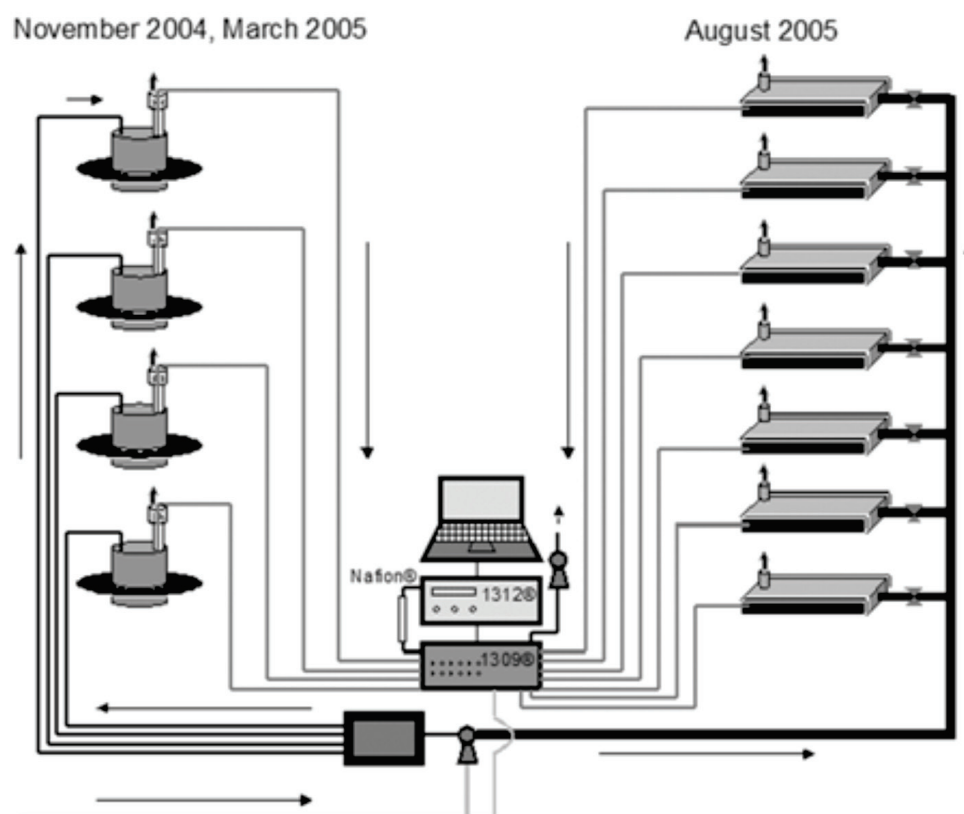


**Figure 2.** Experimental designs in November 2004 and March 2005 (on the left) and in August 2005 (on the right). The floating dynamic chambers were deployed from the shoreline to deeper locations in the littoral zone in Corumbá Reservoir. An air pump drives atmospheric air into the chambers (black lines), exhausted at the chamber outlet vents. A dead volume was used to maintain equal airflows to the chambers in November 2004 and March 2005. In August 2005, the inlet system was reconfigured to a single pipe and individual chamber airflow valves. Another pump and the built-in pump of the photoacoustic trace gas analyzer (Innova 1312<sup>®</sup>) sample air exiting the chambers (gray lines). A multiplexer (Innova 1309<sup>®</sup>) automatically switches among chamber sampling tubes. A nafion<sup>®</sup> tube was fitted between the multiplexer and the gas analyzer. The CH<sub>4</sub> and CO<sub>2</sub> concentrations of the inlet air are measured whenever a chamber sampling cycle is concluded. A portable computer is linked to the Innova 1312<sup>®</sup> through an RS-232 serial connection to operate and store event failure, date, time and gas concentration data.

In 23-28 August 2005 the sampling system was improved and seven dynamic chambers were deployed over depths of 1.0, 2.0, 4.0, 6.0, 8.0, 9.0 and 10m. The chamber design was changed to a rectangular acrylic box of dimensions 15 x 30 x 60cm, with a skirt of 7.5cm below the water surface. A Capex-V2<sup>®</sup> pump drove atmospheric air through a single 150m, 17mm inner diameter pipe (Figure 2). “T” connectors in the pipe split the air and valves at

the chamber inlets to allow regulating the airflow rate at ca. 400ml.min<sup>-1</sup> (Figure 2). 150-m long and 4-mm inner diameter nylon tubes were used to sample gas near the outlet vents and to direct it to the measuring instrumentation.

An infrared photoacoustic gas analyzer (Innova 1312<sup>®</sup>) was used to measure CO<sub>2</sub> and CH<sub>4</sub> concentrations (see Yamulki & Jarvis 1999, Christensen *et al.* 2003a, Abril *et al.* 2006 for

detailed information on gas detection using infrared photoacoustic technology). The instrument was calibrated, including a correction for water vapor. A Permapure Nafion® tube was used to control humidity interference with gas measurements. A multiplexer (Innova 1309®) automatically switched between chamber outlets (and the common inlet) to the Innova 1312® (Figure 2). Gas flux ( $\phi$ , in  $\text{mg}\cdot\text{m}^{-2}\cdot\text{d}^{-1}$ ) was calculated by  $\phi = f(C_o - C_i)/A$ , where  $A$  corresponds to the water surface area ( $\text{m}^2$ ),  $f$  to the airflow ( $\text{m}^3\cdot\text{d}^{-1}$ ) and  $C_o$  and  $C_i$  to the outlet and inlet concentrations. Concentrations given in  $\text{mg}/\text{m}^3$  by the Innova 1312® assume constant temperature ( $25^\circ\text{C}$ ), and the multiplexer corrected for actual air pressure. For each chamber, instantaneous gas fluxes were measured in cycles of  $\sim 10$  minutes on November 2004,  $\sim 5$  minutes on March 2005 and  $\sim 7.5$  minutes on August 2005.

In order to discriminate  $\text{CH}_4$  bubbling from diffusive fluxes, a threshold flux was estimated. This threshold defines an arbitrary baseline, above which episodic  $\text{CH}_4$  bubbling fluxes are noted (Christensen *et al.* 2003a). The baseline thresholds were set to  $60 \text{ mgCH}_4\cdot\text{m}^{-2}\cdot\text{d}^{-1}$  for March 2005, and  $120 \text{ mgCH}_4\cdot\text{m}^{-2}\cdot\text{d}^{-1}$  for August 2005. Because only a single bubbling event was observed in November 2004, a threshold was not set.

#### LIMNOLOGICAL, ATMOSPHERIC AND HYDROLOGIC MEASUREMENTS

Atmospheric (wind speed, solar radiation, air temperature and pressure) and limnological measurements were made with a quasi-continuous monitoring system installed in the pelagic zone of the reservoir (Figure 1). The environmental monitoring system (SIMA) consists of an anchored buoy and a tower, where sensors, electronics, battery and an Argos® type transmitter and antenna were installed to uplink to Brazilian (SCD) and U.S. (NOAA) satellites (Stech *et al.* 2006). Time series were quasi-hourly with small data gaps caused by lack of satellite overpasses or low view angle passes. At two meters below the water surface, an YSI-6600® probe acquired water temperature, pH, dissolved oxygen, chlorophyll *a* and turbidity data. Sensor calibrations were made a day prior to gas measurements. In August 2005, pH data were discarded due to sensor malfunction, and

turbidity and chlorophyll *a* values were below sensor detection limits. The SIMA system was installed in January 2005; in November 2004, only atmospheric temperature and pressure were obtained with a PHTemp101® Madgetech datalogger.

A dataset of hourly water levels measured at the dam was provided by P. Brum and A. Cimbleris (unpublished data). Hourly water level time series were transformed to pressure changes at the sediment-water interface according to  $\Delta p/\Delta t = \rho g (\Delta z/\Delta t) + (\Delta p_a/\Delta t)$ , where  $\rho$ ,  $g$ ,  $\Delta z$  and  $\Delta p_a$  correspond respectively to water density, gravitational acceleration, water level change and atmospheric pressure change.

#### DATA PRE-PROCESSING AND ANALYSIS

Parametric and non-parametric statistical tests were used to determine differences in mean gas fluxes among the sampling sites at distinct depths. Analysis of variances (ANOVA) and Tukey tests were used for  $\text{CO}_2$  and  $\text{CH}_4$  diffusive fluxes, whereas the Kruskal-Wallis test was used for  $\text{CH}_4$  spikes.

To examine correlations among fluxes and limnological and atmospheric data, each time series was set to the same length and time step by a cubic spline algorithm (Press *et al.* 1992). Care was taken by fixing the time step according to gas sampling cycles for each period of measurement. After equalizing length and temporal resolution, gas flux series were further interpolated to fill gaps caused by experimental failures. Gaps were filled with median values of all measurements made during the gap hour (shown in gray in Figures 4, 6, 7 and 8). Except for  $\text{CH}_4$  bubbling time series, high frequency fluctuations were removed by singular value decomposition (Press *et al.* 1992). The lagged covariance matrix was constructed by processing a forward-backward prediction matrix of 40 harmonic signals, restoring only the two first low frequency eigenvalues (harmonics).

Correlations between processed time series were made by means of Pearson or Spearman rank order correlations, depending upon data distribution. Student *t*-tests were performed over processed time series (except for solar radiation) to compare mean differences with respect to day/night measurements and to discriminate mean differences before and after a rainy cold front in March 2005. For  $\text{CH}_4$  bubbling



flux time series, the Mann-Whitney U test was used. Photoperiod (daytime) was assumed to span from 6:00 to 18:00, local time, while the remaining period was considered as nighttime.

## RESULTS

### DEPTH VARIATIONS IN GAS FLUXES

Gas flux measurements from multiple chambers deployed at the same time were well correlated. In November 2004, inter-chamber correlations ranged between 0.69 and 0.89 ( $p < 0.0001$ ) for  $\text{CH}_4$  diffusive fluxes and from 0.83 to 0.94 ( $p < 0.0001$ ) for  $\text{CO}_2$  diffusive fluxes. Figure 3 shows the total  $\text{CH}_4$  fluxes (diffusive + bubbling) at four water depths during three successive days in March 2005. Two “modes” of  $\text{CH}_4$  bubbling emission is discernible: i) large, episodic releases usually at shallower sites and ii) slower releases from deeper sites. While large, episodic  $\text{CH}_4$  releases lack temporal patterns,  $\text{CH}_4$  releases from deeper sites followed a diel cycle, which initiated at about 23:00 and ended at 8:00–10:00 the following morning (Figure 3).

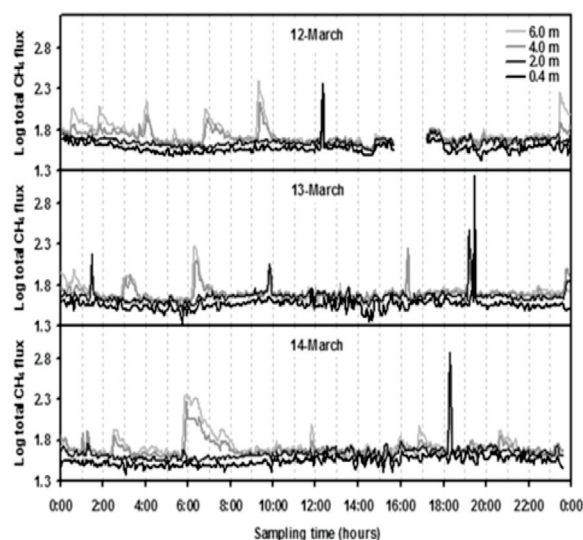


**Figure 3.** Three successive days of the total  $\text{CH}_4$  flux (diffusive + bubbling) given in  $\log \text{mgCH}_4 \cdot \text{m}^{-2} \cdot \text{d}^{-1}$  at shallow (0.4 and 2 m) and deep (4 and 6 m) sites. Note tight spatial and temporal coupling of episodic  $\text{CH}_4$  bubbling especially at deep sites.

The experimental design allowed examining the possible role of water depth in modulating diffusive and bubble fluxes across the water/air interface.

Table 1 provides descriptive statistics of gas fluxes measured in November 2004, March and August 2005. Variances were similar allowing the use of ANOVA to distinguish mean diffusive gas fluxes per depth. Mean  $\text{CH}_4$  diffusion varied significantly with site depths for all sampling periods (ANOVA,  $p < 0.0001$ ). However, the Tukey test did not detect significant differences between mean  $\text{CH}_4$  diffusion for chambers deployed at sites with depths of 3.0 and 3.5 m in November 2004 ( $p < 0.1509$ ). In March 2005, mean  $\text{CH}_4$  diffusive fluxes at all depth sites were significantly different (Tukey test,  $p < 0.0001$ ). In August 2005, significant mean  $\text{CH}_4$  diffusive flux differences among chambers occurred only in some cases, unrelated to the depth of the sampling site (Tukey test).

ANOVA revealed significant mean flux differences among depths for  $\text{CO}_2$  diffusive fluxes, respectively, for November 2004 ( $p < 0.0110$ ), March 2005 ( $p < 0.0001$ ) and August 2005 ( $p < 0.0001$ ). In November 2004, significant mean difference was found only between 1.5 and 3.5 m (Tukey test,  $p < 0.0051$ ). In March 2005, mean difference was not significant between 4 and 6 m (Tukey test,  $p < 0.9675$ ). Significant mean  $\text{CO}_2$  diffusive flux differences among depths occurred only in some cases, unrelated to the depth of the sampling site in August 2005 (Tukey test).

In November 2004, a single bubbling event of  $95 \text{mgCH}_4 \cdot \text{m}^{-2} \cdot \text{d}^{-1}$  was observed in the chamber deployed at 3.5 m water depth (Table 1).  $\text{CH}_4$  bubbling fluxes occurred predominantly during March and August 2005. The Kruskal-Wallis test detected significant differences in  $\text{CH}_4$  bubble fluxes at distinct depths in March and August 2005 (both  $p < 0.0001$ ).

In general, no consistent relation between gas flux and depth was observed.  $\text{CH}_4$  diffusion in November 2004 was inversely related to depth, whereas, in March 2005,  $\text{CH}_4$  diffusion increased with depth.  $\text{CO}_2$  diffusion increased with depth in November 2004 and March 2005. The relation between depth and  $\text{CO}_2$  and  $\text{CH}_4$  diffusive fluxes was more variable in August 2005 (Table 1). Mean  $\text{CH}_4$  bubble fluxes,  $f_b$ , linearly increased up to  $z = 6$  m depth on March 2005 ( $f_b = 1.22z + 0.45$ ,  $r^2 = 0.99$ ) (Table 1).

### SEASONAL DIFFERENCES OF $\text{CH}_4$ AND $\text{CO}_2$ EMISSIONS

A seasonal pattern of gas bubbling and diffusion is evident from November 2004 to August 2005 (Table 1). Mean  $\pm 1$ SD (standard deviation) diffusive fluxes in November 2004, March and August 2005 were respectively  $17 \pm 6.4$ ,  $37 \pm 9$  and  $69 \pm 28 \text{ mg. CH}_4 \cdot \text{m}^{-2} \cdot \text{d}^{-1}$ , and  $59 \pm 398$ ,  $385 \pm 629$  and  $1466 \pm 1223 \text{ mgCO}_2 \cdot \text{m}^{-2} \cdot \text{d}^{-1}$ . For the same months, the mean bubble fluxes were respectively  $0.05 \pm 2$ ,  $4 \pm 45$  and  $505 \pm 1192 \text{ mg. CH}_4 \cdot \text{m}^{-2} \cdot \text{d}^{-1}$ .  $\text{CO}_2$  emission through bubbling was negligible.

### RELATIONSHIPS AMONG GAS FLUXES AND BIOTIC AND ABIOTIC VARIABLES

Processed time series obtained in November 2004 are illustrated in Figure 4. Both  $\text{CO}_2$  and  $\text{CH}_4$  diffusive fluxes slightly increased in parallel with air temperature from 21 to 24 November 2004, but correlations with air temperature were positive for  $\text{CO}_2$  diffusion and negative for  $\text{CH}_4$  diffusion (Table 2). Correlations with pressure changes at the sediment interface were significant for both  $\text{CH}_4$  and  $\text{CO}_2$  diffusive fluxes (Table 2).  $\text{CH}_4$  and  $\text{CO}_2$  diffusive fluxes inversely correlated (Table 2), as  $\text{CO}_2$  ( $\text{CH}_4$ ) fluxes were higher (lower) during the daytime (Table 3). Student t-tests showed that all mean variables were significantly different between day and night (Table 3).

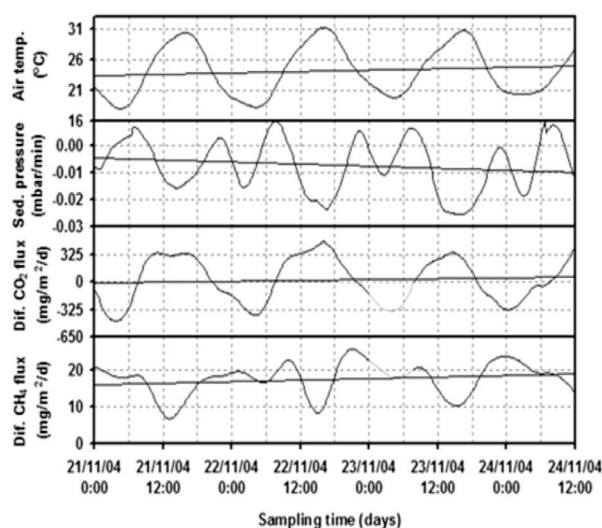


Figure 4. Daily variability of parameters measured in November 2004. The straight lines represent linear trends. Gray curves indicate interpolated data due to system failure.

Time series obtained in March 2005 are illustrated in Figures 5 and 6. A breakpoint related to a rainy cold front appears between 14 and 16 March. Prior to the complete development of the cold front, wind speeds were predominantly below 3 m/s, and after the cold front, the frequency of wind speeds greater than 3 m/s notably increased and both turbidity and chlorophyll *a* increased, while oxygen was redistributed within the water column (Figure 5).

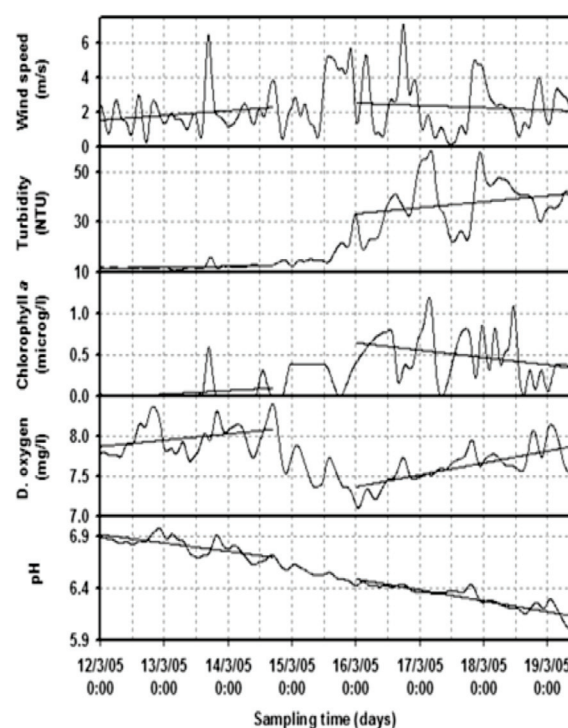
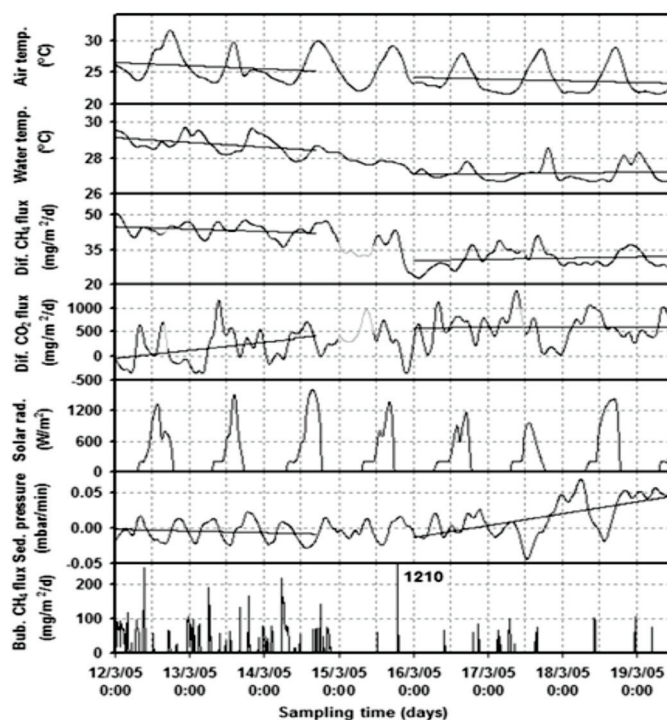


Figure 5. Daily variability of wind speed and limnological parameters measured in March 2005. The straight lines represent linear trends divided into periods prior and after the cold front. Gray curves indicate interpolated data due to system failure.

Prior to the cold front, the air temperature was dropping daily by  $-0.4^\circ\text{C}$  (Figure 6). Following the cold front, mean air temperature remained relatively constant at about  $23.4^\circ\text{C}$ . Water temperature was dropping by  $-0.2^\circ\text{C}$  per day prior to the cold front, and remained between  $27.0$  and  $27.5^\circ\text{C}$  after the cold front. Bubbling intensity and frequency decreased after the cold front.



**Figure 6.** Daily variability of weather, hydrologic and gas flux parameters measured in March 2005. The “1210” number indicates an over scale mean CH<sub>4</sub> bubbling flux. The straight lines represent linear trends divided into periods prior and following the cold front. Gray curves indicate interpolated data due to system failure.

The differences between means before and after the cold front were all statistically significant (Table 4). This was also the case between day and night periods, except for chlorophyll *a* (*t*-test,  $p < 0.1764$ ) and for CH<sub>4</sub> bubble flux (Mann-Whitney U test,  $p < 0.3243$ ) following the cold front (Table 4). Wind

speed was moderately correlated with CH<sub>4</sub> and CO<sub>2</sub> diffusive fluxes, as well as to CH<sub>4</sub> bubble fluxes (Table 2). The pressure change at the sediment interface was inversely correlated with CH<sub>4</sub> diffusive and bubble fluxes, while directly correlated with CO<sub>2</sub> diffusive fluxes (Table 2).

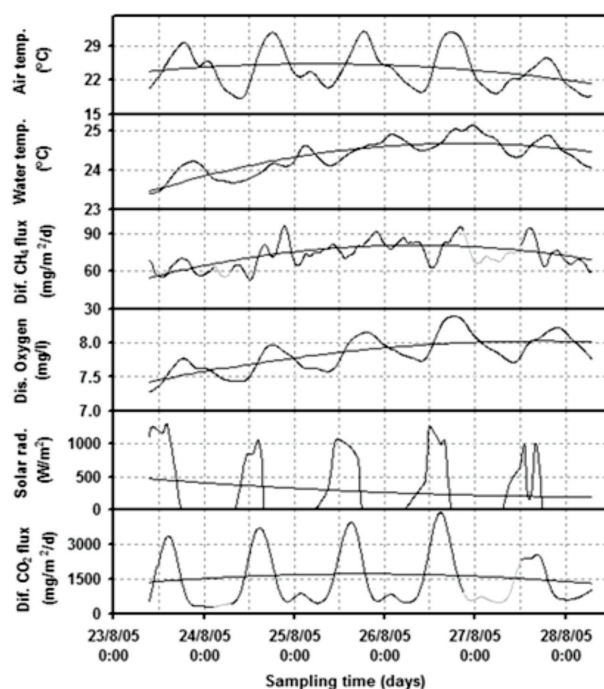


**Figure 7.** Daily variability of weather, hydrologic and gas flux parameters measured in August 2005. The curves represent second order trends. Gray curves indicate interpolated data due to system failure.



The time series obtained in August 2005 are illustrated in Figures 7 and 8. Water and air temperatures covaried with dissolved oxygen and  $\text{CH}_4$  and  $\text{CO}_2$

diffusive fluxes. Wind speeds were generally lower than those observed in March 2005.  $\text{CH}_4$  bubble fluxes were exceptionally high in August 2005.

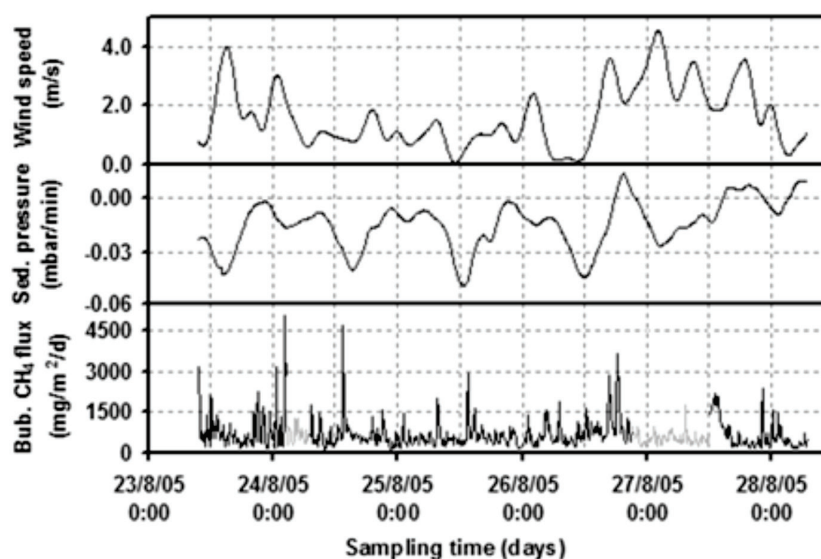


**Figure 8.** Daily variability of wind, pressure change at sediment and gas flux parameters measured in August 2005. Gray curves indicate interpolated data due to system failure.

Mean differences between day and night were statistically significant for all variables considered (Table 5). Wind speed was unrelated to  $\text{CH}_4$  and  $\text{CO}_2$  diffusive fluxes, and to  $\text{CH}_4$  bubble fluxes (Table 2). The changes in pressure at the sediment interface were inversely correlated with  $\text{CO}_2$  diffusive fluxes and  $\text{CH}_4$  bubble fluxes, and directly correlated with  $\text{CH}_4$  diffusive fluxes (Table 2).

## DISCUSSION

### TEMPORAL AND SPATIAL DIFFERENCES IN GAS FLUXES

In the littoral zone of Central American reservoirs,  $\text{CH}_4$  bubbling fluxes were inversely related to the sampling depth (Keller & Stallard 1994, Joyce & Jewell 2003). In this study, mean  $\text{CH}_4$  bubbling in March 2005 increased from 0.4 to 6 m (Table 1), whereas  $\text{CH}_4$  bubbling was independent of the depth of the sampling site in August 2005. We did observe large, episodic  $\text{CH}_4$  releases especially at shallower sites in March 2005 (Figure 3). However, other biotic and abiotic mechanisms, such as shear stress (Joyce & Jewell 2003), sediment pressure change (Rosenqvist *et al.* 2002) or the methanogenesis/methanotrophy

ratio could be responsible for variability in bubble flux.

Warmer periods and regions usually have enhanced  $\text{CH}_4$  emissions because bacterial methanogenesis varies with temperature (Christensen *et al.* 2003b).  $\text{CO}_2$  emissions should also increase with water and air temperature due to the increase in methanotrophy and transfer velocities in the mixed layer (MacIntyre *et al.* 2001, Jonsson *et al.* 2003). During the three periods of measurements, gas diffusion usually followed air and water temperatures (Figures 4-8). However, mean water temperature was significantly (t-test,  $p < 0.0001$ ) higher in March 2005, whereas mean  $\text{CH}_4$  and  $\text{CO}_2$  diffusive fluxes were respectively 2 and 4-fold higher in August 2005 (see Tables 4 and 5).

In the Everglades,  $\text{CH}_4$  emissions during daytime were low due to dissolved oxygen increases (King 1990); oxygen originating from photosynthesis may have enhanced methanotrophy (Lima *et al.* 2005b). The results herein shown are in agreement with these findings, as daytime  $\text{CO}_2$  fluxes were higher than those observed during the night (Table 3). In March 2005, methanotrophy appeared to be enhanced by photosynthetic oxygen production and water column mixing due to the cold front.



The lack of correlation between wind speed and gas fluxes on the time scale of minutes (Table 2) may be explained by the following: i) the dynamic chamber method provides a constant airflow inside the chambers; ii) the chamber shielded the surface from wind and iii) wind speed was measured hourly about 1 km from the gas sampling sites. However, we did observe an effect of wind on gas effluxes due to a rainy cold front (Figure 5). Thermocline deepening and mixing induced by wind energy has been observed to disrupt stratification and enhance gas exchange (Engle & Melack 2000, MacIntyre *et al.* 2001).

Engle & Melack (2000) observed large  $\text{CH}_4$  bubble and diffusion emissions during the passage of a cold front at an Amazon lake. We could not measure  $\text{CH}_4$  emission during the passage of the cold front due to system failure (see interpolated data in Figure 6). Nonetheless, we could verify that after the passage of the cold front both frequency and magnitude of bubble fluxes significantly lowered (Table 5 and Figure 6). Such change may arise from a large  $\text{CH}_4$  release and oxidation during the cold front passage (not measured) and the subsequent re-oxygenation of the water column (see changes in wind speed and dissolved oxygen in Figure 5 and sediment pressure in Figure 6). Between 16 and 17 March, an increase in dissolved oxygen (+66%) occurred in the hypolimnion (F. Roland & D. E. Cesar, personal communication) and could have resulted in suppression of methanogenesis and enhancement of methanotrophy. Moreover, the decrease in pH (Figure 5) and the increase in alkalinity (+16%) (F. Roland & D. E. Cesar, personal communication) indicated a possible increase in dissolved  $\text{CO}_2$  derived from the enhancement of methanotrophy.

It is well documented that pressure drops at the sediment interface can trigger  $\text{CH}_4$  bubble releases (Mattson & Likens 1990, Rosenqvist *et al.* 2002, Huttunen *et al.* 2003). Such phenomenon, also induced by wind and shear stress (Keller & Stallard 1994, Joyce & Jewell 2003), can cause strong spatial correlation in bubble releases. A bubble pulse may occur whenever sufficient increase in bubble volume occurs due to pressure drop (Mattson & Likens 1990). A decrease in pressure at the sediment interface sufficient to increase bubble volume can induce

sediment disruption (Johnson *et al.* 2002) and bubble releases. Bubble volume may also expand as the number of moles of  $\text{CH}_4$  increases in sediments due to methanogenesis. Suppression of  $\text{CH}_4$  bubbling can be associated with increase in pressure at the sediment interface (Figure 6), but bubbling was barely noticeable in November 2004 despite sediment depressurization (Figure 4). In August 2005 bubbling was intense and unaffected by the increase in hydrostatic pressure that started at about 20:00 on August 26<sup>th</sup> (Figure 8), possibly because methanogenesis was high. At that time the mean areal concentration in the sediment surface integrated for the 0-4cm was  $918\text{mgCH}_4\cdot\text{m}^{-2}$ , about twice as much as that measured in the two previous sampling periods (D. Abe, unpublished data, 2006). Therefore, bubble releases can be modulated by a combined effect of the rate of methanogenesis and changes in sediment pressure.

#### METHANOGENESIS AND METHANOTROPHY

At least 50% of methanogenesis in Corumbá Reservoir was via acetate reduction, whereas only 17% was accounted by  $\text{H}_2/\text{CO}_2$  reduction (D. Abe, unpublished data, 2006). The carbon isotope ratio in methane bubbles was  $\delta^{13}\text{C}-\text{CH}_4 = -57 \pm 4.3\text{‰}$  ( $n = 8$ , August 2005) (Bergier, unpublished data), further evidence for the dominance of acetoclastic methanogenesis (Whiticar 1999).

$\text{CH}_4$  releases from the water surface to the atmosphere are not equivalent to sediment/water fluxes, since a fraction of the diffusing  $\text{CH}_4$  is converted into  $\text{CO}_2$  by methanotrophic bacteria under aerobic conditions. Although variable, methanotrophy can consume a considerable portion of  $\text{CH}_4$ . Methanotrophy can take place at the oxic, upper part of sediment or within the water column. In Lake Washington, about 50% of the  $\text{CH}_4$  flux was oxidized to  $\text{CO}_2$  in the upper 7mm of the sediments and the remainder escaped into the water column (Kuivila *et al.* 1988). In Lake Constance, ca. 93% of the  $\text{CH}_4$  produced was oxidized within the oxic layer of sediment by aerobic methanotrophic bacteria (Frenzel *et al.* 1990). Dissolved  $\text{CH}_4$  oxidation can be dependent on water column depth. Although  $\text{CH}_4$  concentrations in sediments were equivalent, the amount of dissolved  $\text{CO}_2$  was higher in Tucuruí

Reservoir (eastern Amazon, mean depth of 20m) than in Samuel Reservoir (western Amazon, mean depth of 6 m), because methanotrophy is favored in deep reservoirs (Lima, 2005). For Lobo-Broa Reservoir (southern Brazil), about 90% of  $\text{CH}_4$  can be oxidized either at the sediment/water interface or in the water column (Abe *et al.* 2005). In Corumbá Reservoir, diel  $\text{CH}_4$  and  $\text{CO}_2$  diffusive fluxes were inversely correlated, except in August 2005 (Table 2) probably due to the difficulty to effectively discriminate diffusion from bubble fluxes under very intense bubbling conditions (Figure 8). Nonetheless, for the three periods of measurement,  $\text{CO}_2$  diffusive fluxes were usually higher during daylight, generally peaking between 11:00 and 17:00. In Tucuruí and Samuel reservoirs, sunlight stimulated oxygen production via photosynthesis, which in turn activated methanotrophy (Lima *et al.* 2005b). Therefore, we presume that during the three periods of measurement a non-negligible fraction of  $\text{CO}_2$  effluxes might correspond to methanotrophy taking place within the aquatic ecosystem.

#### HETEROTROPHY AND CARBON SOURCES

Lake metabolism, also called net ecosystem production (NEP), is the difference between gross primary production and respiration. In general, aquatic ecosystems respire more organic carbon than they produce through photosynthesis and are, therefore, net heterotrophic (Cole, 1999). Refractory organic carbon can become more available to the aquatic food web by photo-oxidation, which can produce low molecular weight organic acids, such as acetate (Corin *et al.* 1998). Dissolved organic carbon (DOC) in aquatic ecosystems is usually allochthonous, and  $\text{CH}_4$  accumulation in the hypolimnion can be correlated with epilimnetic and hypolimnetic DOC, but not necessarily with primary production (Houser *et al.* 2003). Autotrophy within water bodies depends on light and nutrient supply, and, as nutrient availability increases during the flood pulse (Junk *et al.* 1989), conditions are generally favorable for algal growth. Based on these general observations, we hypothesize that seasonal methanogenesis in Corumbá Reservoir is possibly linked to a “heterotrophic pulse”, as there is a time lag between net autotrophy in the rainy

season, and the peak in  $\text{CH}_4$  and  $\text{CO}_2$  emissions in the dry season, linked to periods of net heterotrophy.

Nutrients and organic carbon are introduced in the reservoir by the flood pulse and by primary production. While in transit, the labile portions of DOC may undergo biological degradation through aerobic pathways (Mayorga *et al.* 2005), leaving only the refractory fraction that may be deposited in the sediment. Other sources of refractory carbon in the sediments are the pre-impoundment biomass, such as soil carbon and dead trees. Hence, net autotrophy is probably highest during the flood pulse. In the dry season, terrigenous organic matter and water inflows are less at Corumbá Reservoir. Transparency is elevated and primary production is lower, as indicated by turbidity and chlorophyll *a* in August 2005 (Table 5). From March to August 2005, the water level dropped by more than 10 meters, allowing a portion of the still flooded sediment to be more exposed to solar radiation. Consequently, it is possible that photo-oxidation of the carbon in the surficial sediments, exposed to sunlight during receding water periods, could contribute to high rates of methanogenesis in the littoral zone.

#### CONCLUSIONS

The continuous measurement technique allowed observing a significant difference between greenhouse gas fluxes during day and night periods.  $\text{CO}_2$  emissions may partially result from diel methanotrophy within the water column.

Gas fluxes varied with the depth of the sampling sites in the littoral zone, even though spatial or temporal patterns were not seasonally consistent. Both the rate of methanogenesis and changes in sediment pressure jointly affected  $\text{CH}_4$  emission through bubbling. Rainy, cold fronts redistributed dissolved oxygen within the water column, reduced  $\text{CH}_4$  bubbling and enhanced  $\text{CO}_2$  evasion. Seasonality in gas fluxes might be primarily modulated by heterotrophy and hydrologic pulses being out of phase.

**ACKNOWLEDGEMENTS:** Furnas Centrais Elétricas S.A., supervised by the National Agency for Electric Energy (ANEEL), supported this R&D Project entitled “Carbon balance in Furnas reservoirs”. Ivan Bergier thanks Dr. Nicolas Soumis, Dr. Bruce Forsberg, Dr. John Melack, Dr. Frédéric Guérin, Dr. Reinaldo Rosa, Dr. Fabio Roland, Dr. Arcilan Assireu, Dr. Jean Ometto, Dr. João Lorenzetti, Dr. José Stech and Dr. Donato Abe for contributions to the development of the present manuscript.

## REFERENCES

- ABE, D.S.; ADAMS, D.D.; GALLI, C.V.S.; SIKAR, E. & TUNDISI, J.G. 2005. Sediment greenhouse gases (methane and carbon dioxide) in the Lobo-Broa Reservoir, São Paulo State, Brazil: Concentrations and diffuse emission fluxes for carbon budget considerations. *Lakes and Reservoirs Research and Management*, 10: 201-210.
- ABRIL, G.; GUÉRIN, F.; RICHARD, S.; DELMAS, R.; GALY-LACAUX, C.; GOSSE, P.; TREMBLAY, A.; VARFALVY, L.; SANTOS, M.A. & MATVIENKO, B. 2005. Carbon dioxide and methane emissions and the carbon budget of a 10-year old tropical reservoir (Petit Saut, French Guiana). *Global Biogeochemical Cycles*, 19: doi:10.1029/2005GB002457
- ABRIL, G.; RICHARD, S. & GUÉRIN, F. 2006. In situ measurements of dissolved gases ( $\text{CO}_2$  and  $\text{CH}_4$ ) in a wide range of concentrations in a tropical reservoir using an equilibrator. *Science of the Total Environment*, 354: 246-251.
- CHRISTENSEN, T.R.; PANIKOV, N.; MASTEPANOV, M.; JOABSSON, A.; STEWARD, A.; ÖQUIST, M.; SOMMERKORN, M.; REYNAUD, S. & SVENSSON, B. 2003a. Biotic controls on  $\text{CO}_2$  and  $\text{CH}_4$  exchange in wetlands - a closed environment study. *Biogeochemistry*, 64: 337-354.
- CHRISTENSEN, T.R.; EKBERG, A.; STRÖM, A.; MASTEPANOV, M.; PANIKOV, N.; ÖQUIST, M.; SVENSSON, B.H.; NYKÄNEN, H.; MARTIKAINEN, P.J. & OSKARSSON, H. 2003b. Factors controlling large scale variations in methane emissions from wetlands. *Geophysical Research Letters*, 30: 1414, doi:10.1029/2002GL016848
- COLE, J.J. 1999. Aquatic microbiology for ecosystem scientists: New and recycled paradigms in ecological microbiology. *Ecosystems*, 2: 215-225.
- CORIN, N.; BACKLUND, P. & WIKLUND, T. 1998. Bacterial growth in humic waters exposed to UV-radiation and simulated sunlight. *Chemosphere*, 36: 1947-1958.
- CRILL, P.M.; BARTLETT, K.B.; WILSON, J.O.; SEBACHER, D.I.; HARRISS, R.C.; MELACK, J.M.; MACINTYRE, S.; LESACK, L. & SMITH-MORRILL, L. 1988. Tropospheric methane from an Amazonian floodplain lake. *Journal of Geophysical Research*, 93: 1564-1570.
- DUCHEMIN, E.; LUCOTTE, M. & CANUEL, R. 1999. Comparison of static chamber and thin boundary layer equation methods for measuring greenhouse gas emission from large water bodies. *Environmental Science and Technology*, 33: 350-357.
- DUCHEMIN, E.; LUCOTTE, M.; ST. LOUIS, V. & CANUEL, R. 2002. Hydroelectric reservoirs as an anthropogenic source of greenhouse gases. *World Resource Review*, 14: 334-353.
- ENGLE, D. & MELACK, J.M. 2000. Methane emissions from an Amazon floodplain lake: enhanced release during episodic mixing and during falling water. *Biogeochemistry*, 51: 71-90.
- FANG, C. & MONCRIEFF, J.B. 1998. An open-top chamber for measuring soil respiration and the influence of pressure difference on  $\text{CO}_2$  efflux measurements. *Functional Ecology*, 12: 319-325.
- FELISBERTO, S.A. & RODRIGUES, L. 2004. Periphytic desmids in Corumbá Reservoir, Goiás, Brazil: genus *Cosmarium* Corda. *Brazilian Journal of Biology* 64, 141-150.
- FRENZEL, P.; THEBRATH, B. & CONRAD, R. 1990. Oxidation of methane in the oxic surface layer of a deep lake sediment (Lake Constance). *FEMS Microbiol Ecology* 73: 149-158.
- GUÉRIN, F.; ABRIL, G.; RICHARD, S.; BURBAN, B.; REYNOUARD, C.; SEYLER, P. & DELMAS, R. 2006. Methane and carbon dioxide emissions from tropical reservoirs: significance of downstream rivers. *Geophysical Research Letters*, 33: L21407, doi:10.1029/2006GL027929
- HOUSER, J.N.; BADE, D.L.; COLE, J.J. & PACE, M.L. 2003. The dual influences of dissolved organic carbon on hypolimnetic metabolism: organic substrate and photosynthetic reduction. *Biogeochemistry*, 64: 247-269.
- HUTTUNEN, J.T.; ALM, J.; LIIKANEN, A.; JUUTINEN, S.; LARMOLA, T.; HAMMAR, T.; SILVOLA, J. & MARTIKAINEN, P.J. 2003. Fluxes of methane, carbon dioxide and nitrous oxide in boreal lakes and potential anthropogenic effects on the aquatic greenhouse gas emissions. *Chemosphere*, 52: 609-621.
- JOHNSON, B.D.; BOUDREAU, B.P.; GARDINER, B.S. & MAASS, R. 2002. Mechanical response of sediments to bubble growth. *Marine Geology*, 187: 347-363.
- JONSSON, A.; KARLSSON, J. & JANSSON, M. 2003. Sources of carbon dioxide supersaturation in clearwater and humic lakes in Northern Sweden. *Ecosystems*, 6: 224-235.
- JOYCE, J. & JEWELL, P.W. 2003. Physical controls on methane ebullition from reservoirs and lakes. *Environmental Engineering Geosciences*, 9: 167-178.

- JUNK, W.J.; BAYLEY, P.B. & SPARKS, R.E. 1989. The flood pulse concept in river-floodplain systems. *Canadian Special Publication on Fisheries and Aquatic Sciences*, 106: 110-127.
- KELLER, M. & STALLARD, R.F. 1994. Methane emission by bubbling from Gatun Lake, Panama. *Journal of Geophysical Research*, 99: 8307-8319.
- KING, G.M. 1990. Regulation by light of methane emissions from a wetland. *Nature*, 345: 513-515.
- KUIVILA, K.M.; MURRAY, J.W.; DEVOL, A.H.; LIDSTROM, M.E. & REIMERS, C.E. 1988. Methane cycling in the sediments of Lake Washington. *Limnology and Oceanography*, 33: 571-581.
- LIMA, I.B.T. 2005. Biogeochemical distinction of methane releases from two Amazon hydroreservoirs. *Chemosphere*, 59: 1697-1702.
- LIMA, I.B.T.; MAZZI, E.A.; CARVALHO, J.C.; OMETTO, J.P.H.B.; RAMOS, F.M.; STECH, J.L. & NOVO, E.M.L.M. 2005a. Photoacoustic/dynamic chamber method for measuring greenhouse gas fluxes in hydroreservoirs. *Verhandlungen des Internationalen Verein Limnologie*, 29: 603-606.
- LIMA, I.B.T.; OMETTO, J.P.H.B.; MAZZI, E.A. & NOVO, E.M.L.M. 2005b. Circadian release of methane from Amazon hydroreservoirs. *Verhandlungen des Internationalen Verein Limnologie*, 29: 580-582.
- LIMA, I.B.T.; RAMOS, F.M.; BAMBACE, L.A.W. & ROSA, R.R. 2008. Methane emissions from large dams as renewable energy resources: a developing nation perspective. *Mitigation and Adaptation Strategies for Global Change*, 13: 196-206.
- LISS, P.S. & SLATER, P.G. 1974. Flux of gases across the air-sea interface. *Nature*, 247: 181-184.
- MACINTYRE, S.; EUGSTER, W. & KLING, G.W. 2001. The critical importance of buoyancy flux for gas flux across the air-water interface. Pp. 135-139. In: M.A. Donelan, W.M. Drennan, E.S. Saltzman & R. Wanninkhof (eds.). Gas transfer at water surfaces. AGU Geophysical Monograph Series, Washington DC. 383p.
- MATTSON, M.D. & LIKENS, G.E. 1990. Air pressure and methane fluxes. *Nature*, 347: 718-719.
- MATTEWS, C.D.; ST. LOUIS, V. & HESSLEIN, R. 2003. Comparison of three techniques used to measure diffusive gas exchange from sheltered aquatic surfaces. *Environmental Science and Technology*, 37: 772-780.
- MAYORGA, E.; AUFDENKAMPE, A.K.; MASIELLO, CA.; KRUSCHE, A.V.; HEDGES, I.J.; QUAY, P.D.; RICHEY, J.E. & BROWN, T.A. 2005. Young organic matter as a source of carbon dioxide outgassing from Amazonian rivers. *Nature*, 436: 538-541.
- NAY, S.M.; MATTSON, K.G. & BORMANN, B.T. 1994. Biases of chamber methods for measuring soil CO<sub>2</sub> efflux demonstrated with a laboratory apparatus. *Ecology*, 75: 2460-2463.
- PRESS, W.H.; FLANNERY, B.P.; TEUKOLSKY, S.A. & VETTERLING, W.T. 1992. *Numerical recipes in FORTRAN: the art of scientific computing*. Cambridge University Press, Cambridge. 1486p.
- RAMOS, F.M.; LIMA, I.B.T.; ROSA, R.R.; MAZZI, E.A.; CARVALHO, J.C.; RASERA, M.F.F.L.; OMETTO, J.P.H.B.; ASSIREU, A.T. & STECH, J.L. 2006. Extreme event dynamics in methane ebullition fluxes from tropical reservoirs. *Geophysical Research Letters*, 33: L21404, doi:10.1029/2006GL027943
- ROSENQVIST, A.; FORSBERG, B.R.; PIMENTEL, T.P.; RAUSTE, Y.A. & RICHEY, J.E. 2002. The use of spaceborne radar data to model inundation patterns and trace gas emissions in the Central Amazon floodplain. *International Journal of Remote Sensing*, 7: 1303-1328.
- STECH, J.L.; LIMA, I.B.T.; NOVO, E.M.L.M.; SILVA, C.M.; ASSIREU, A.T.; LORENZZETTI, J.A.; CARVALHO, J.C.; BARBOSA, C.C. & ROSA, R.R. 2006. Telemetric monitoring system for meteorological and limnological data acquisition. *Verhandlungen des Internationalen Verein Limnologie*, 29: 1747-1750.
- ST. LOUIS, V.L.; KELLY, C.A.; DUCHEMIN, E.; RUDD, J.W.M. & ROSENBERG, D.M. 2000. Reservoir surfaces as sources of greenhouse gases to the atmosphere: a global estimate. *Bioscience*, 50: 766-775.
- WHITICAR, M.J. 1999. Carbon and hydrogen isotope systematics of bacterial formation and oxidation of methane. *Chemical Geology*, 161: 291-314.
- YAMULKI, S. & JARVIS, S.C. 1999. Automated chamber technique for gaseous flux measurements: evaluation of a photoacoustic infrared spectrometer-trace gas analyzer. *Journal of Geophysical Research*, 104: 5463-5469.

Submetido em 24/11/2010

Aceito em 14/07/2011



**Table 1.** Variability of greenhouse gas diffusive and bubble fluxes at Corumbá Reservoir.

	Depth of Sampling site	Methane diffusive flux mgCH <sub>4</sub> .m <sup>-2</sup> .d <sup>-1</sup>	Number of Observations N	Methane bubbling flux mgCH <sub>4</sub> .m <sup>-2</sup> .d <sup>-1</sup>	Number of bubble events	Number of Observations N	Carbon dioxide diffusive flux mgCO <sub>2</sub> .m <sup>-2</sup> .d <sup>-1</sup>	Number of Observations N
Nov. 2004	1.5 m	21 ± 6	472	0.0	0	472	13 ± 390	472
	3.0 m	18 ± 6	472	0.0	0	472	63 ± 412	472
	3.5 m	17 ± 8	471	0.2 ± 4.0 <sup>a</sup>	1	472	98 ± 406	472
	6.0 m	14 ± 5	472	0.0	0	472	64 ± 378	472
Mean	3.5 m	17 ± 6		0.05 ± 2.19			59 ± 398	
March 2005	0.4 m	32 ± 7	1981	1 ± 31	6	1987	186 ± 546	1987
	2.0 m	37 ± 9	1972	3 ± 74	15	1987	379 ± 597	1987
	4.0 m	41 ± 9	1863	5 ± 32	124	1987	482 ± 651	1987
	6.0 m	38 ± 9	1802	8 ± 29	185	1987	491 ± 666	1987
Mean	3.1 m	37 ± 9		4.4 ± 45			385 ± 629	
August 2005	1.0 m	57 ± 26	389	307.8 ± 664.8	300	689	1608 ± 1407	689
	2.0 m	78 ± 25	66	1435 ± 2468	623	689	1571 ± 1294	689
	4.0 m	86 ± 24	136	336.0 ± 401.1	553	689	1153 ± 1056	689
	6.0 m	85 ± 26	93	421.8 ± 470.7	596	689	1527 ± 1263	689
	8.0 m	76 ± 25	258	214.1 ± 331.9	431	689	1463 ± 1034	689
	9.0 m	65 ± 26	345	331.0 ± 1198	344	689	1378 ± 1256	689
	10 m	72 ± 27	155	492.3 ± 678.6	534	689	1561 ± 1148	689
Mean	7.1 m	69 ± 28		505.4 ± 1192			1466 ± 1223	

<sup>a</sup> Computed from a single bubbling event of 95.1mgCH<sub>4</sub>.m<sup>-2</sup>.d<sup>-1</sup>.

**Table 2.** Correlations between variables from Corumbá Reservoir.

	November 2004		March 2005			August 2005		
	Methane diffusive flux <sup>a</sup>	Carbon dioxide diffusive flux <sup>a</sup>	Methane diffusive flux <sup>a</sup>	Methane bubbling flux <sup>b</sup>	Carbon dioxide diffusive flux <sup>a</sup>	Methane diffusive flux <sup>a</sup>	Methane bubbling flux <sup>b</sup>	Carbon dioxide diffusive flux <sup>a</sup>
Wind speed <sup>a</sup>	-	-	-0.14	-0.13	-0.19	-0.06 <sup>c</sup>	-0.05 <sup>c</sup>	0.03 <sup>c</sup>
Air temperature <sup>a</sup>	-0.61	0.92	0.50	0.07 <sup>c</sup>	-0.30	0.38	0.16	0.46
Water temperature <sup>a</sup>	-	-	0.80	0.32	-0.63	0.57	-0.01 <sup>c</sup>	-0.05 <sup>c</sup>
Solar radiation <sup>b</sup>	-	-	0.04 <sup>c</sup>	-0.14	0.42	-0.04 <sup>c</sup>	0.19	0.65
Dissolved oxygen <sup>a</sup>	-	-	0.58	0.18	0.23	-	-	-
pH <sup>a</sup>	-	-	0.79	0.32	-0.57	-	-	-
Turbidity <sup>b</sup>	-	-	-0.73	-0.31	0.51	-	-	-
Chlorophyll a <sup>b</sup>	-	-	-0.68	-0.32	0.44	-	-	-
Sediment pressure change <sup>a</sup>	0.54	-0.42	-0.34	-0.11	0.14	0.20	-0.15	-0.52
CO <sub>2</sub> diffusive flux <sup>a</sup>	-0.59	-	-0.41	-	-	0.04 <sup>c</sup>	-	-

<sup>a</sup> Pearson correlations, significance level  $p < 0.0001$ .<sup>b</sup> Spearman rank correlations, significance level  $p < 0.0001$ .<sup>c</sup> not significant.**Table 3.** Day (6:00-18:00) versus night (18:00-6:00) differences for variables acquired in November 2004.

	Air temperature (°C) <sup>a</sup>		Sediment pressure change (mbar.min <sup>-1</sup> ) <sup>b</sup>		Methane diffusive flux (mgCH <sub>4</sub> .m <sup>-2</sup> .d <sup>-1</sup> ) <sup>a</sup>		Carbon dioxide diffusive flux (mgCO <sub>2</sub> .m <sup>-2</sup> .d <sup>-1</sup> ) <sup>a</sup>	
	Day	Night	Day	Night	Day	Night	Day	Night
N	256	244	256	244	256	244	256	244
Min.	18.6	18.0	-0.025	-0.023	6.79	14.3	-305	-459
Mean	26.5	21.9	-0.008	-0.006	15.1	20.1	222	-170
Max.	31.3	30.0	0.009	0.005	22.6	25.6	470	342

<sup>a</sup> Day vs. night mean difference is significant at  $p < 0.0001$  (t-test).<sup>b</sup> Day vs. night mean difference is significant at  $p < 0.0568$  (t-test).

**Table 4.** Day (6:00-18:00) versus night (18:00-6:00) differences and effects of the cold front on variables acquired in March 2005.

	Prior to the cold front (PCF) <sup>a,c</sup>						After the cold front (ACF) <sup>b,c</sup>									
	Day			Night			Day			Night						
	N	Min.	Mean	Max.	N	Min.	Mean	Max.	N	Min.	Mean	Max.	N	Min.	Mean	Max.
Wind speed (m/s)	378	0.3	2.1	6.5	319	0.8	1.8	3.7	449	0.2	1.6	7.1	447	0.5	3	7
Air temperature (°C)	378	23	26.2	31.6	319	23.6	25.5	31.5	449	21.6	24.4	28.9	447	21.6	23.1	28.5
Water temperature (°C)	378	27.8	28.4	28.9	319	28.5	29.2	29.7	449	26.7	27	27.8	447	26.7	27.3	28.6
Dissolved oxygen (mg.l <sup>-1</sup> )	378	7.7	7.9	8.4	319	7.8	8	8.4	449	7.2	7.6	8	447	7.1	7.7	8.1
pH	378	6.6	6.8	6.9	319	6.7	6.9	7	449	6	6.3	6.4	447	6.1	6.3	6.5
Turbidity (NTU)	378	11.2	12.4	16.1	319	10.8	11.9	15.3	449	22.1	35.4	47.5	447	19	39.7	58.4
Chlorophyll a (mg.l <sup>-1</sup> )	378	0	0.1	0.6	319	0	0	0.3	449	0	0.5	1.1	447	0.1	0.5	1.2
Sediment pressure change (mbar.min <sup>-1</sup> )	378	-0.028	-0.007	0.018	319	-0.024	-0.002	0.024	449	-0.043	0.008	0.07	447	-0.014	0.024	0.069
Methane diffusive flux (mgCH <sub>4</sub> .m <sup>-2</sup> .d <sup>-1</sup> )	378	36	43.2	47.6	319	36.3	43.8	50.8	449	25.7	30.6	41.1	447	22.7	31.8	39
Methane bubbling flux (mgCH <sub>4</sub> .m <sup>-2</sup> .d <sup>-1</sup> )	378	0	15.5	246.6	319	0	22	218.3	449	0	2.3	103.7	447	0	1.5	105.7
Carbon dioxide diffusive flux (mgCO <sub>2</sub> .m <sup>-2</sup> .d <sup>-1</sup> )	378	-200.9	396.9	1165.3	319	-350.6	-53.2	546.6	449	50.4	765.5	1362.9	447	34.3	423.4	794.4

<sup>a</sup> PCF. The differences between day vs. night means are all significant (t-test) for wind speed ( $p < 0.0002$ ), CH<sub>4</sub> diffusive flux ( $p < 0.0044$ ) and to the remaining variables ( $p < 0.0001$ ); CH<sub>4</sub> bubbling flux (Mann-Whitney U test,  $p < 0.0002$ ).

<sup>b</sup> ACF. The differences between day vs. night means are all significant (t-test,  $p < 0.0001$ ), except for chlorophyll a (t-test,  $p < 0.1764$ ) and CH<sub>4</sub> bubbling flux (Mann-Whitney U test,  $p < 0.3243$ ).

<sup>c</sup> The differences between PCF vs. ACF means are all significant (t-test,  $p < 0.0001$ ); CH<sub>4</sub> bubbling flux (Mann-Whitney U test,  $p < 0.0001$ ).

**Table 5.** Day (6:00–18:00) versus night (18:00–6:00) differences for variables acquired in August 2005.

	Day				Night			
	N	Min.	Mean	Max.	N	Min.	Mean	Max.
Wind speed (m/s)	490	0.1	1.5	4	510	0.2	1.8	4.5
Air temperature (°C)	490	18.2	23.9	31.7	510	18.6	24.7	31.9
Water temperature (°C)	490	23.4	24.2	25	510	23.7	24.5	25.1
Dissolved oxygen (mg.l <sup>-1</sup> )	490	7.3	7.8	8.4	510	7.4	7.9	8.4
pH	-	-	n.m.	-	-	-	n.m.	-
Turbidity (NTU)	-	-	b.d.l.	-	-	-	b.d.l.	-
Chlorophyll a (mg.l <sup>-1</sup> )	-	-	b.d.l.	-	-	-	b.d.l.	-
Sediment pressure change (mbar.min <sup>-1</sup> )	490	-0.05	-0.022	0.01	510	-0.027	-0.008	0.014
Methane diffusive flux (mgCH <sub>4</sub> .m <sup>-2</sup> .d <sup>-1</sup> )	490	26.8	43	57.8	510	33.1	46.2	58.2
Methane bubbling flux (mgCH <sub>4</sub> .m <sup>-2</sup> .d <sup>-1</sup> )	490	245.3	619.7	1485.8	510	230	512.1	1405.7
Carbon dioxide diffusive flux (mgCO <sub>2</sub> .m <sup>-2</sup> .d <sup>-1</sup> )	490	423.5	2164.9	4376.1	510	292.4	779.6	2686

The differences between day vs. night means are significant (t-test) to all variables ( $p < 0.0001$ ); CH<sub>4</sub> bubbling flux (Mann-Whitney U test,  $p < 0.0001$ ).

n.m. – not measured.

b.d.l. - below detection limit.